# Supporting information

## The inner heterogeneity of zeolite crystals

*Yanfeng Shen, [a] Zhengxing Qin, *[a] Shunsuke Asahina, [b] Natsuko Asano, [b] Guanqun Zhang, [c] Shuya Qian, [a] Yanhang Ma, [c] Zifeng Yan, [a] Xinmei Liu, [a] and Svetlana Mintova*[a,d]*

[a] Y. Shen, Dr. Z. Qin, S. Qian, Prof. Z. Yan, Prof. X. Liu, Prof. S. Mintova
State Key Laboratory of Heavy Oil Processing, College of Chemical Engineering
China University of Petroleum (East China)
No. 66, West Changjiang Road, Huangdao District, Qingdao, China, 266580
E-mail: zhengxing.qin@upc.edu.cn; svetlana.mintova@ensicaen.fr

[b] Dr. S. Asahina, Dr. N. Asano
SEM Application Team
JEOL Ltd.
3-1-2 Musashino, Akishima, Tokyo, Japan, 196-8558

[c] Dr. G. Zhang, Dr. Y. Ma
School of Physical Science and Technology
ShanghaiTech University
393 Middle Huaxia Road, Shanghai, China, 201210

[d] Prof. S. Mintova,
Laboratoire Catalyse et Spectrochimie
Normandie Univ, ENSICAEN, UNICAEN, CNRS
6 Bd Marchal Juin, Caen, France, 14000

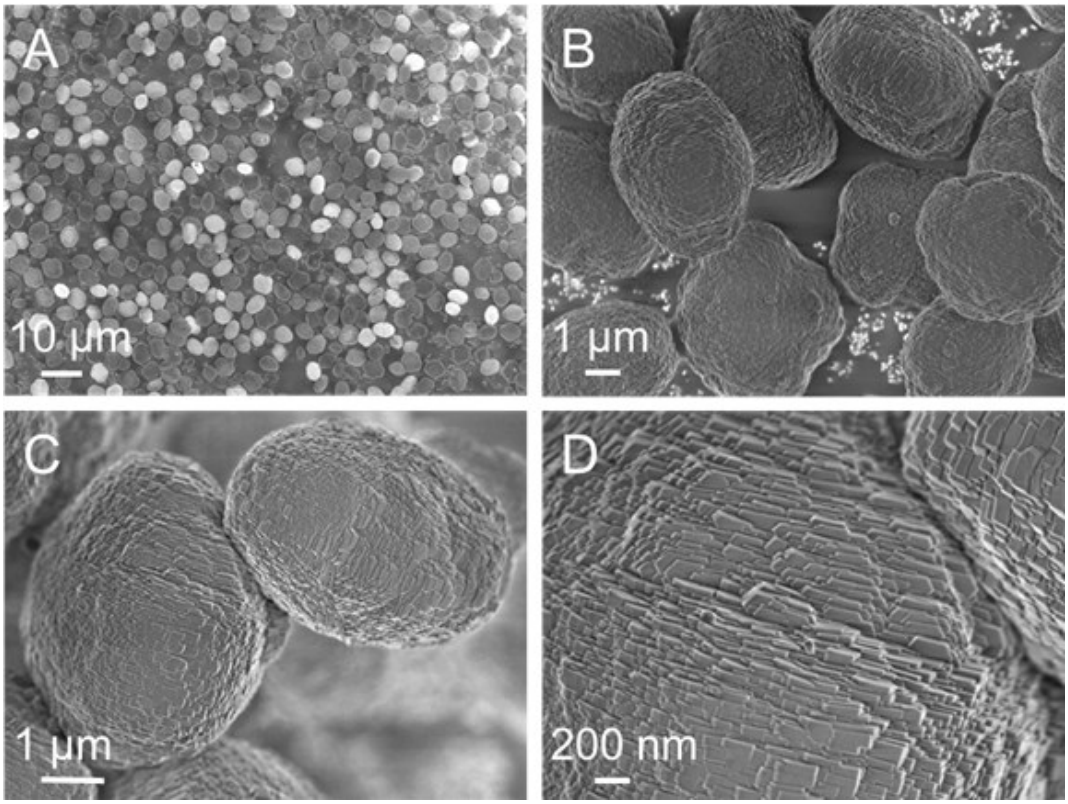


**Figure S1.** SEM images of $Z_p$ (parent ZSM-5 zeolite).

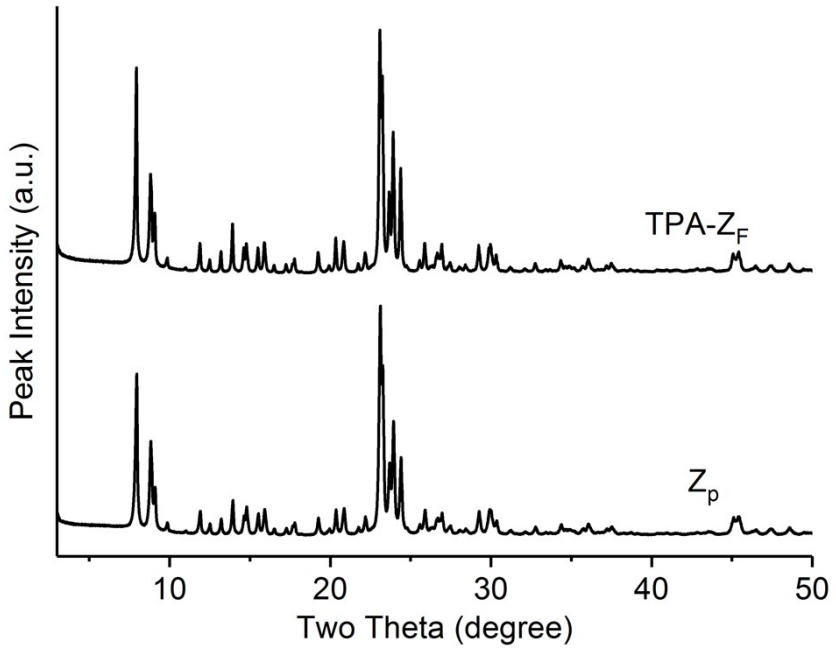


**Figure S2** XRD patterns of the $Z_p$ (parent) and TPA-$Z_F$ ($NH_4F$ treated) ZSM-5 zeolite samples.

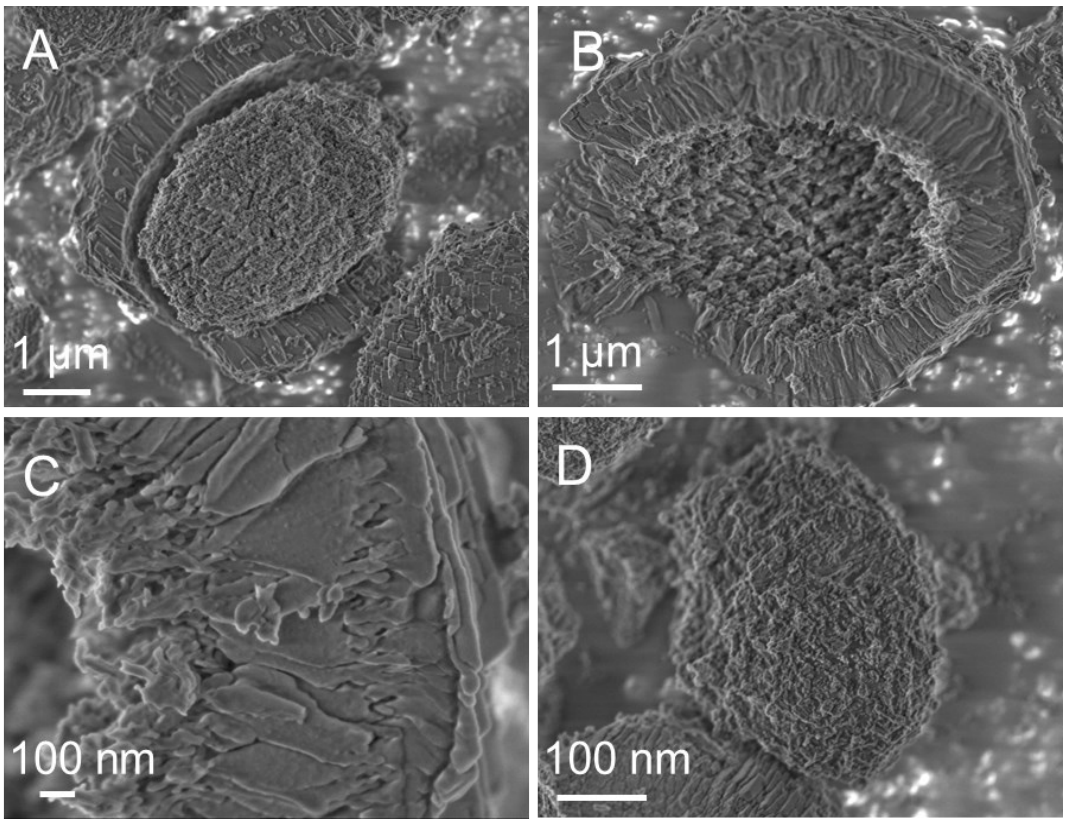


**Figure S3** SEM images of sample TPA-$Z_F$ showing the core-shell structure (A), the empty shell (B), the structural details of the shell (C) and the naked core part (D).

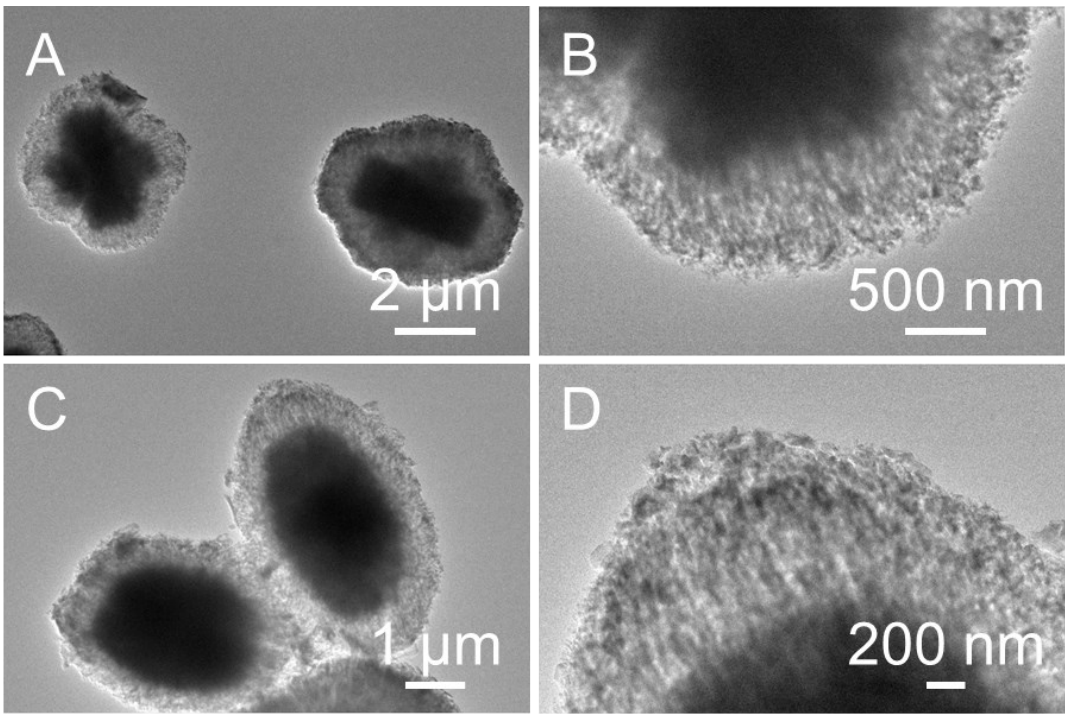


**Figure S4** TEM images showing the either rectangular (A) or elliptical shaped (C) core part ("egg-yolk") of sample TPA-$Z_F$. Figures S4B and S4D highlight the very porous nature of the outer layer ("egg-white") and the much less porous nature of the core part.

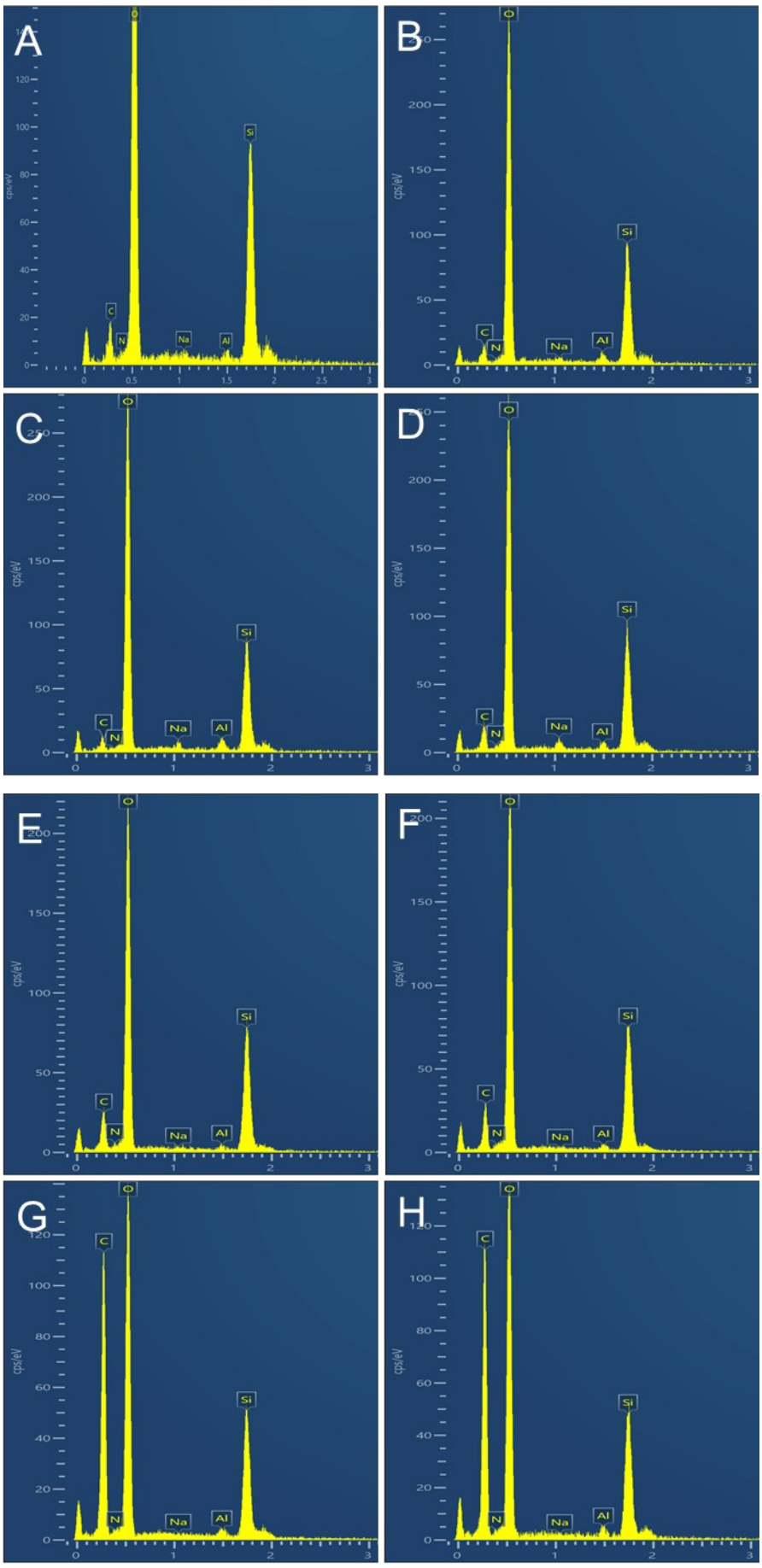


**Figure S5** SEM-EDX spectra showing the point analysis results for zones 1 (A), 2 (B), 3 (C) and 4 (D) indicated in Figure 4A; zones 1 (E), 2 (F), 3 (G) and 4 (H) indicated in Figure 4C.

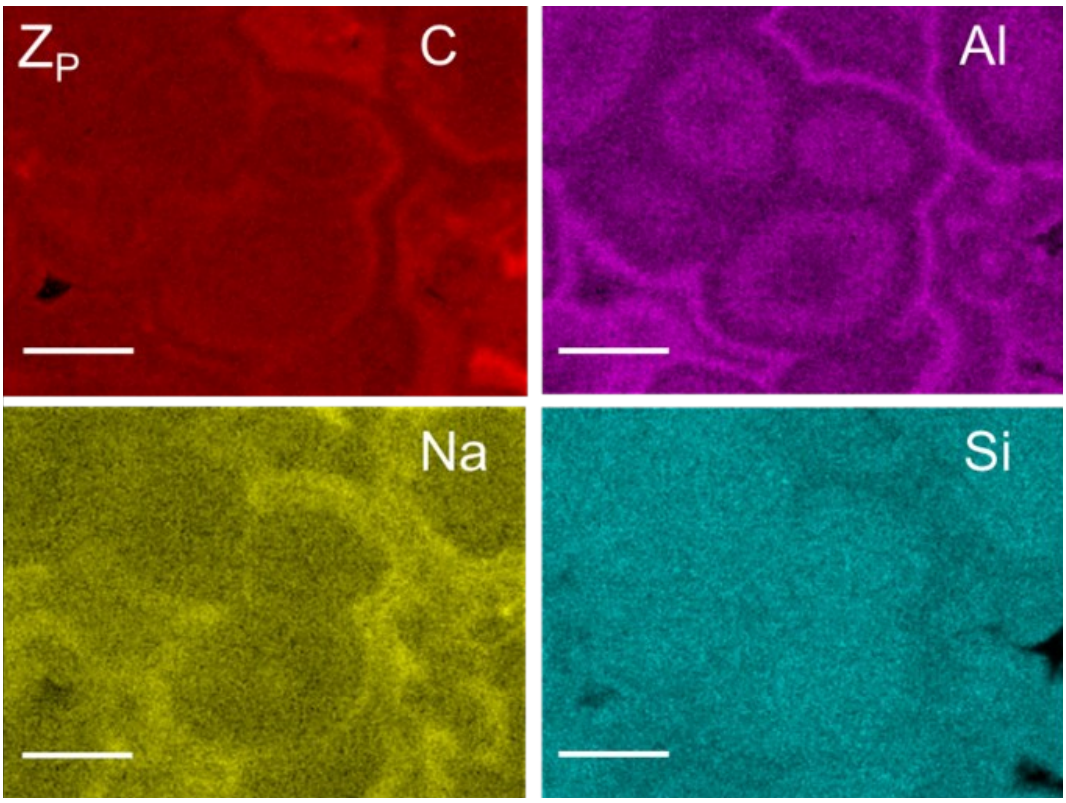


**Figure S6** SEM EDX mappings of the $Z_P$ (parent ZSM-5) zeolite crystals. Scale bar = 2.5 μm.

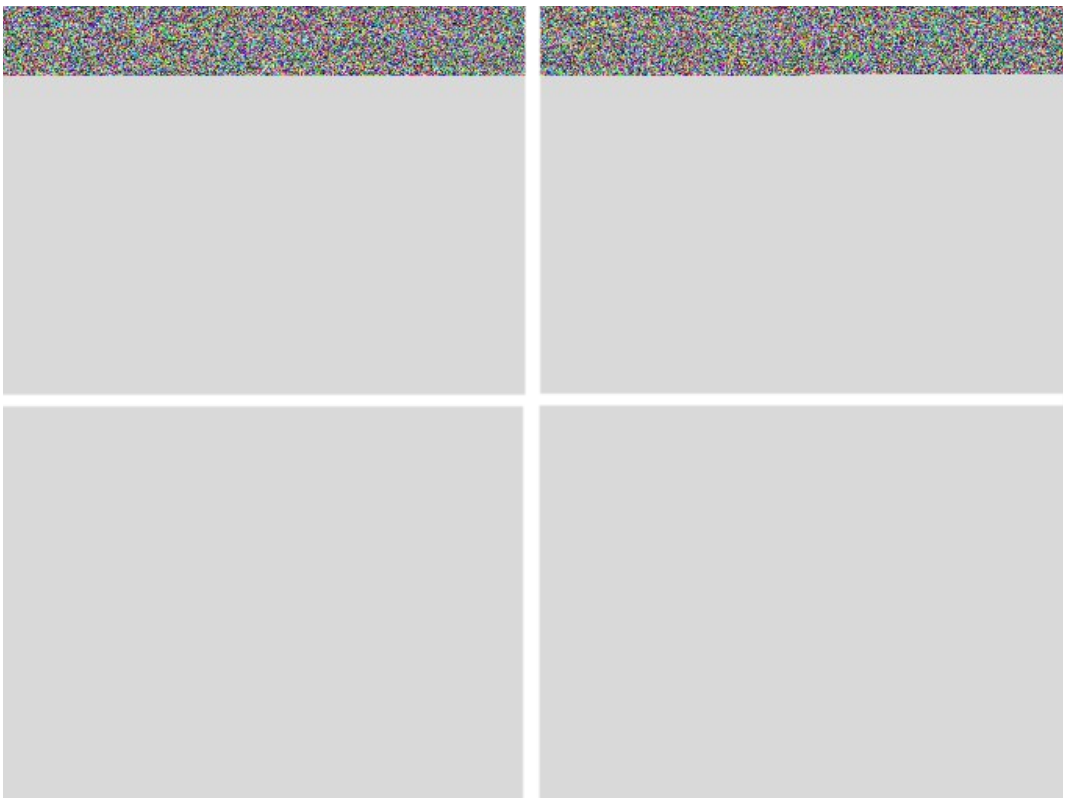

**Figure S7** SEM EDX mappings of the TPA-$Z_F$ ($NH_4F$ treated ZSM-5) zeolite crystals. Scale bar = 2.5 μm.

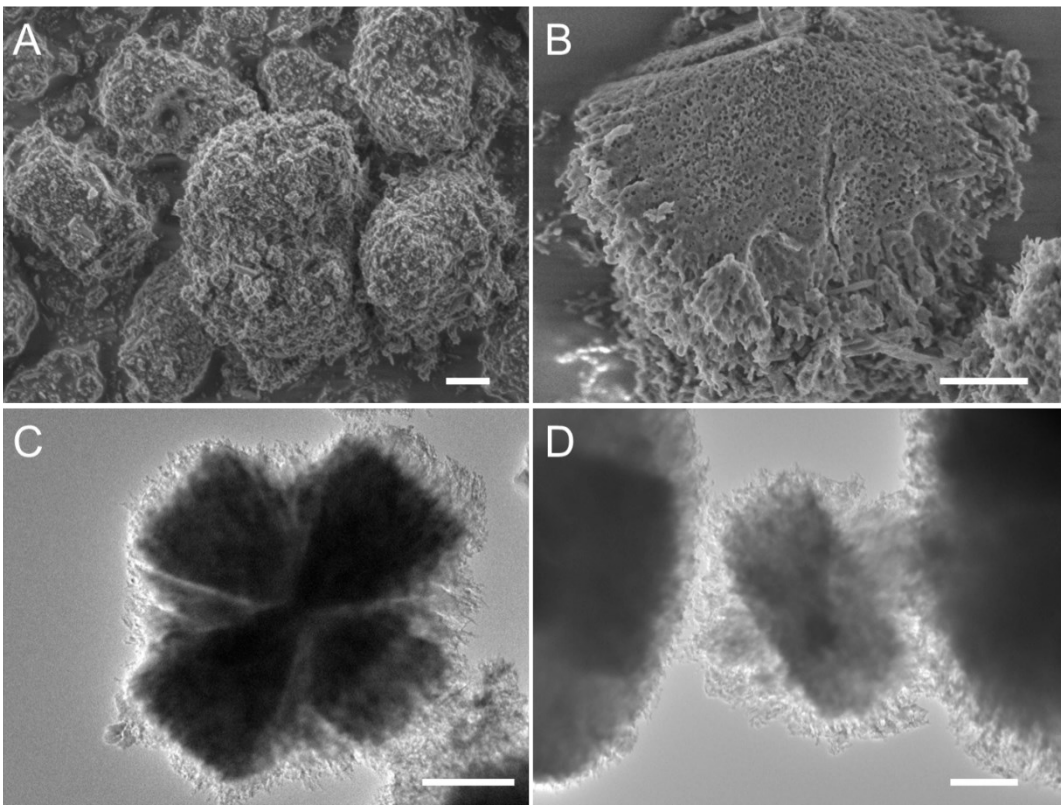


**Figure S8** SEM (A, B) and TEM (C, D) images of calcined ZSM-5 samples (no $TPA^+$) treated by $NH_4F$. (A, C, D) The sample was collected after 1 h treatment with $NH_4F$. (B) The sample was collected after 2 h treatment with $NH_4F$. Scale bar: 1 μm in A and C; 500 nm in B and D.

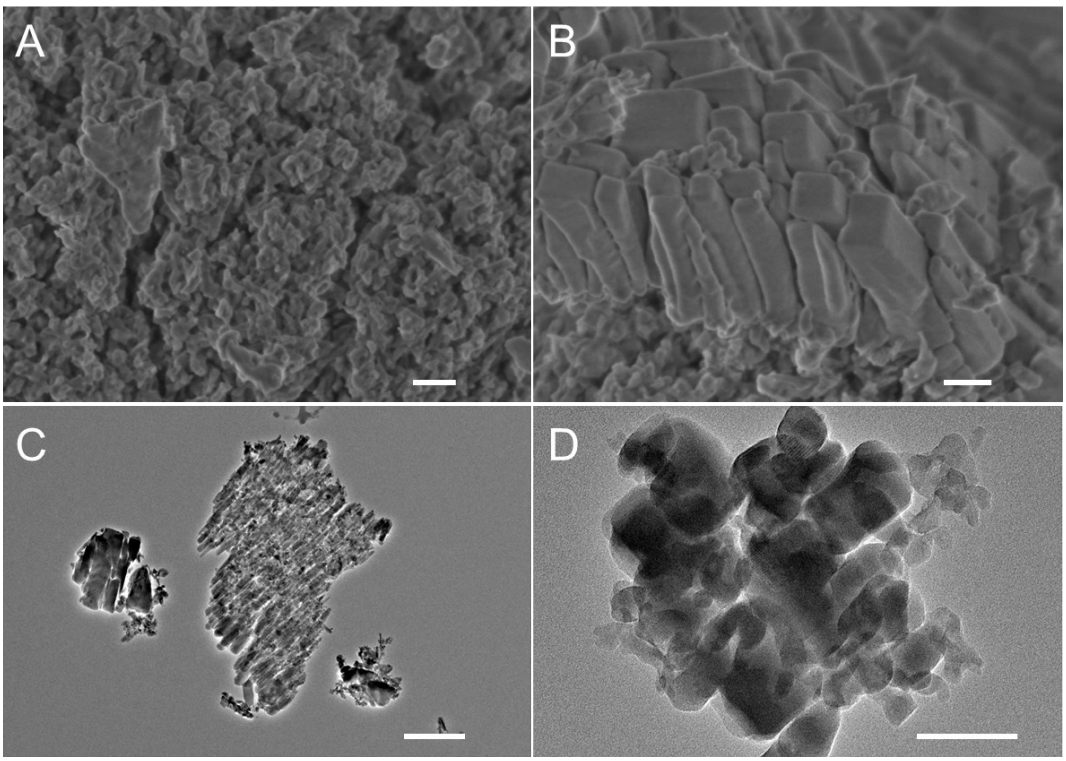


**Figure S9** SEM (A, B) and TEM (C, D) images showing the surface details of the $R_2$ (A) and $R_1$ (B-D) zones of sample TPA-$Z_F$. Scale bar: 100 nm in A, B and D; 500 nm in C.

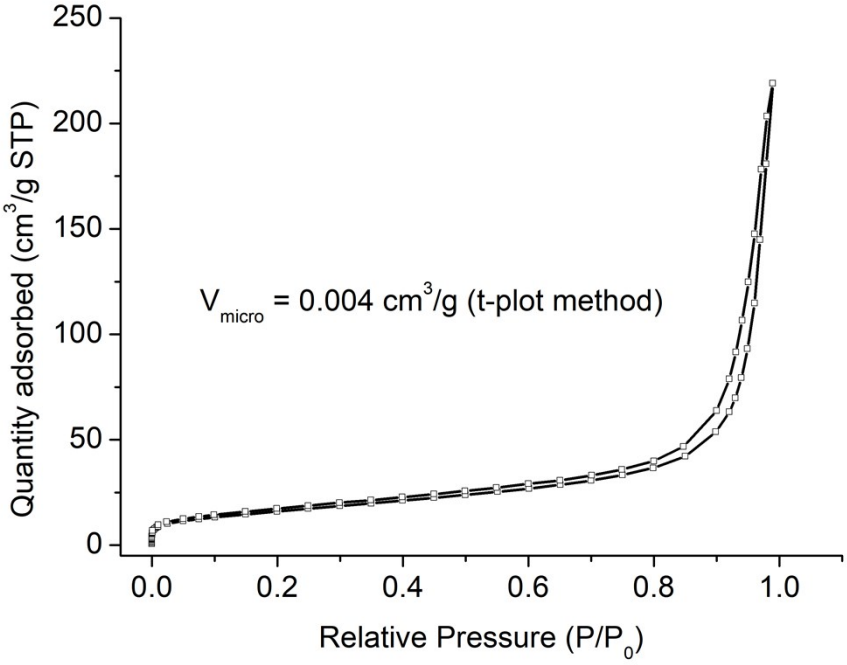


**Figure S10** $N_2$ (77K) physisorption isotherms of $Na^+$ exchanged TPA-$Z_F$ zeolite.

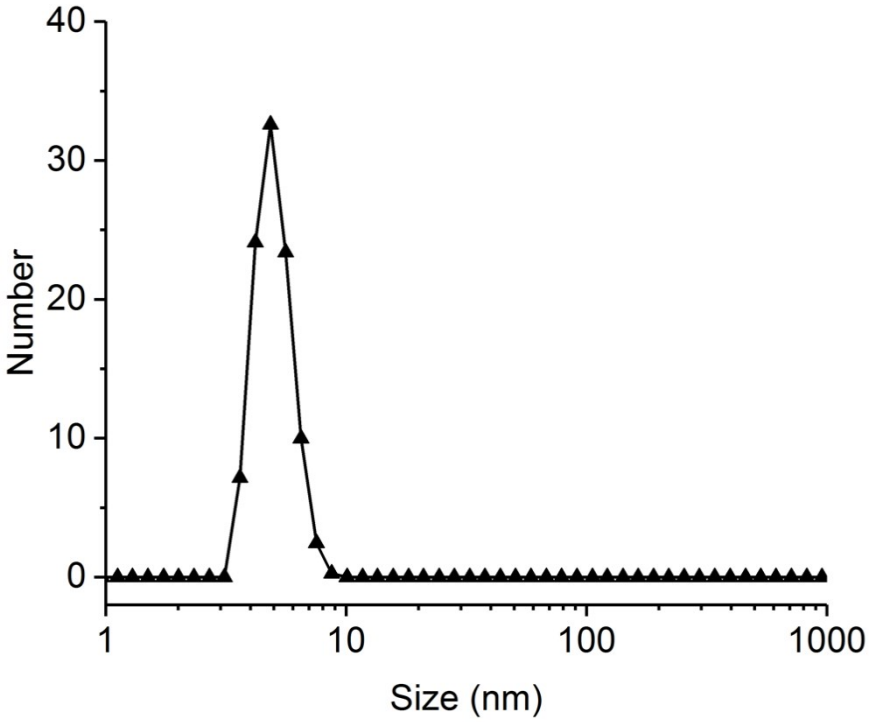


**Figure S11** Particles size distribution of the aluminosilicate precursor gel determined by dynamic light scattering (DLS).

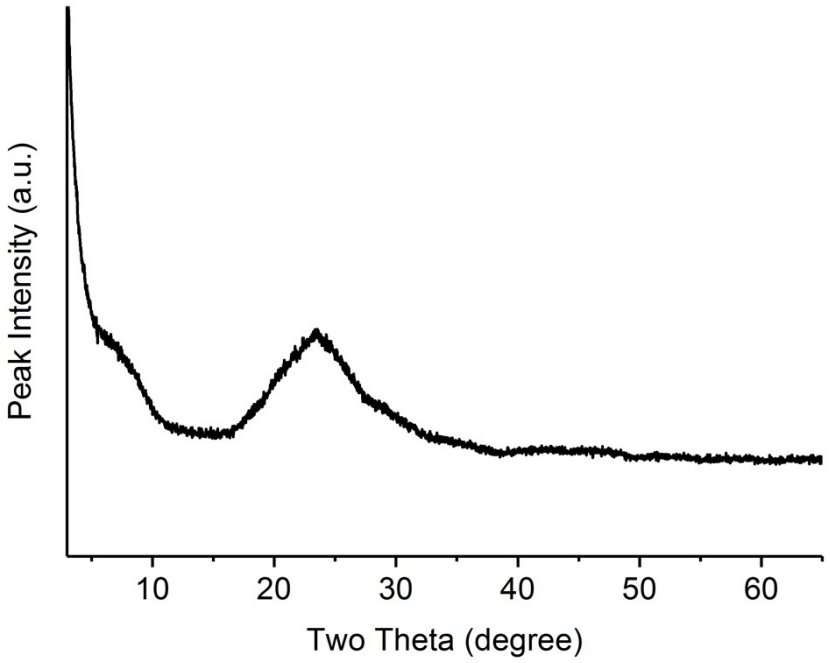


**Figure S12** XRD pattern of the sample collected after hydrothermal synthesis at 443 K for 2 h.

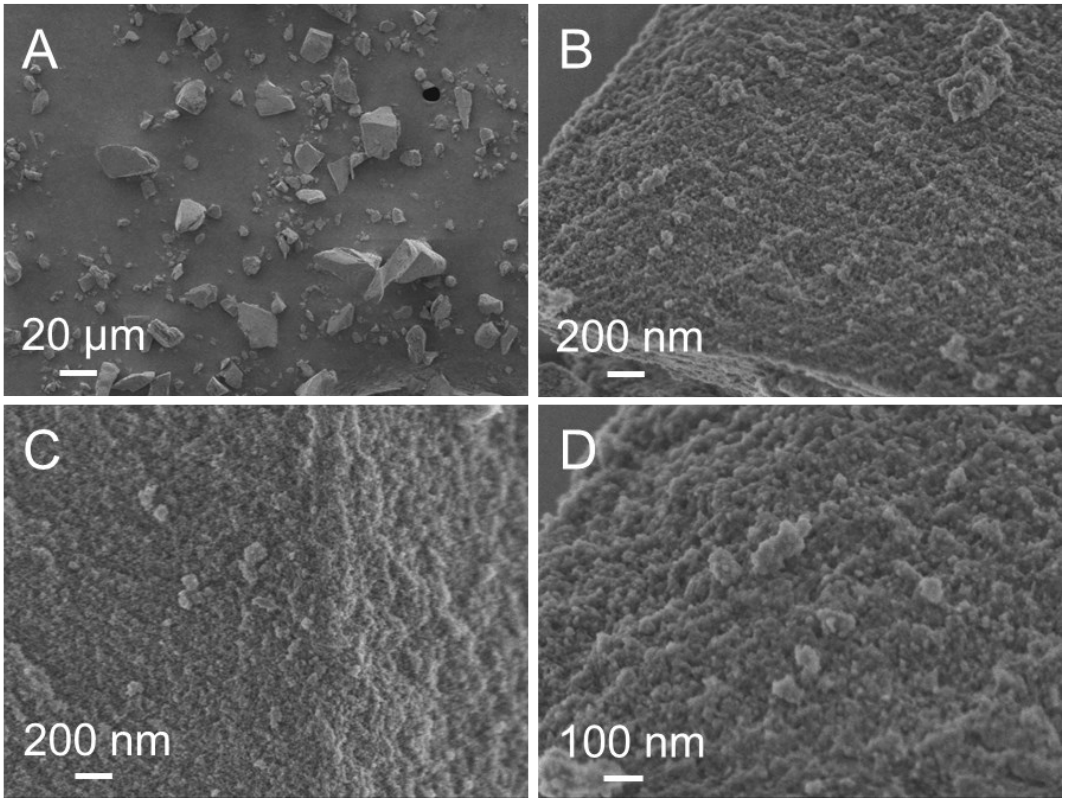


**Figure S13** SEM images of samples obtained after hydrothermal synthesis at 443 K for 2 h.

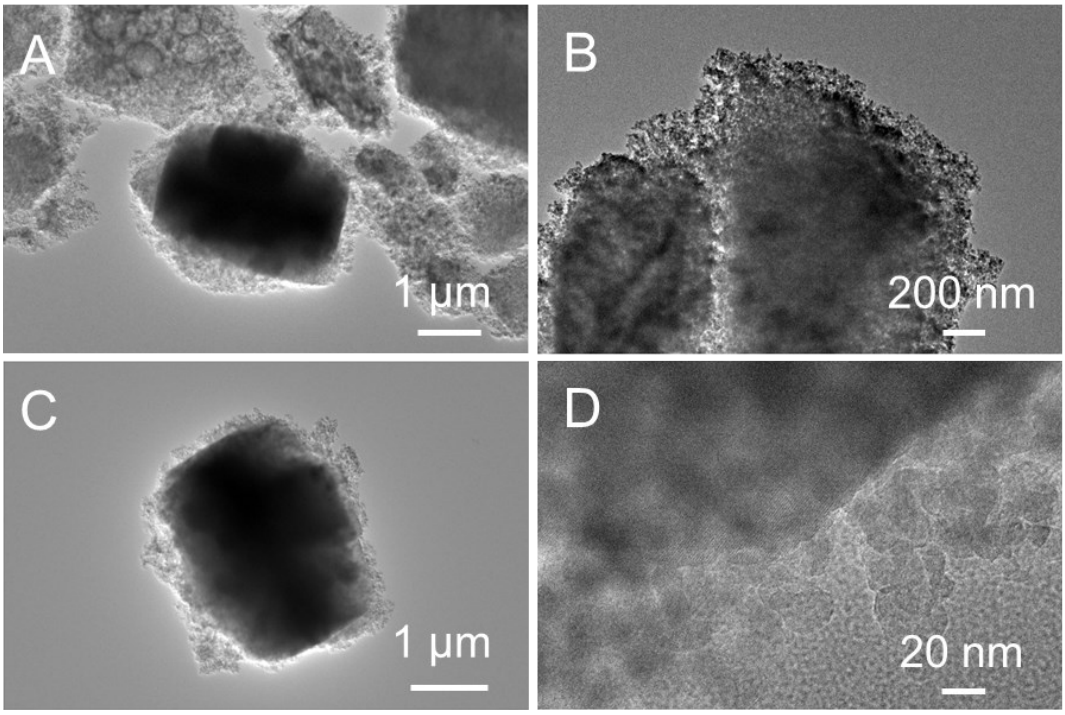


**Figure S14** TEM images of sample obtained after hydrothermal synthesis at 443 K for 4 h.

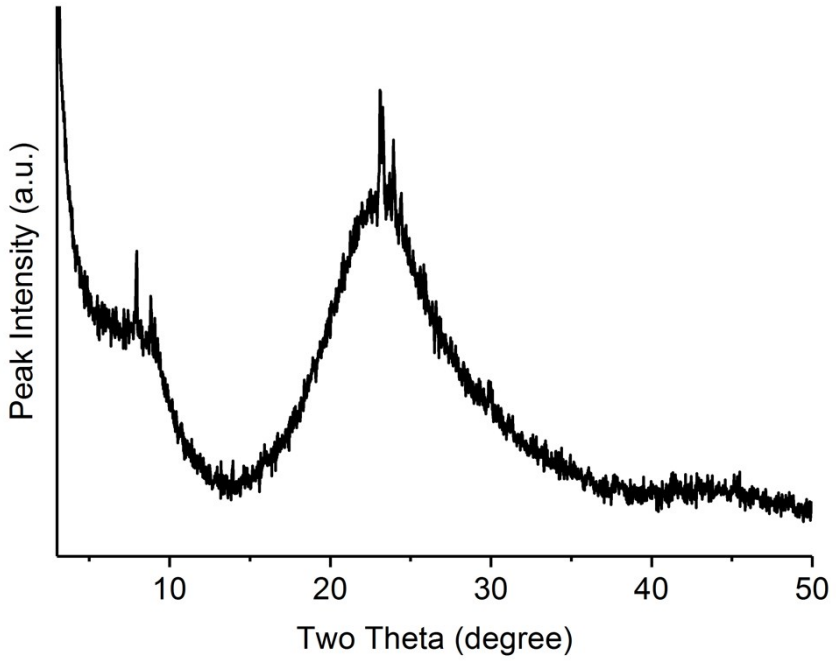


**Figure S15** XRD pattern of the sample obtained after hydrothermal synthesis at 443 K for 4 h.

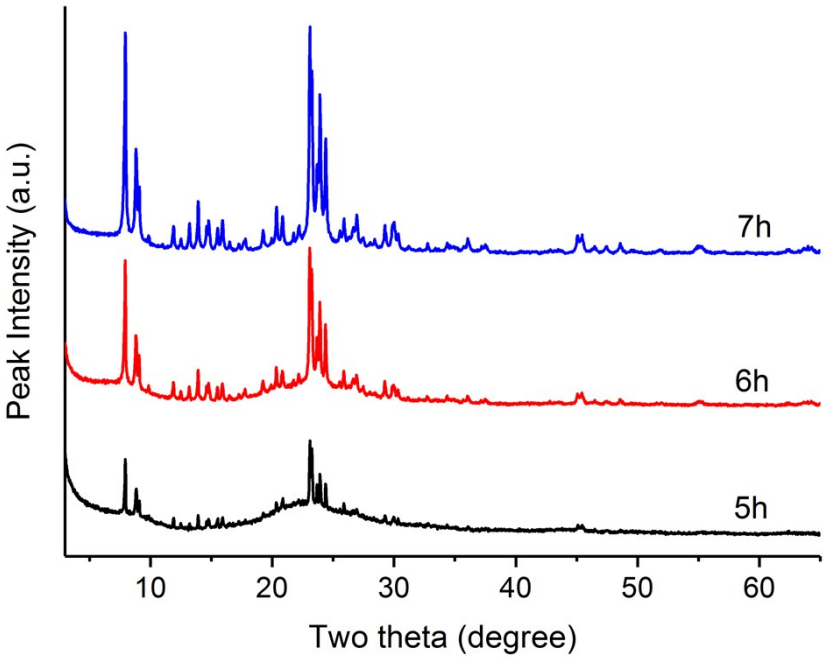


**Figure S16** XRD patterns of the sample obtained after hydrothermal synthesis at 443 K for 5 h, 6h and 7h.

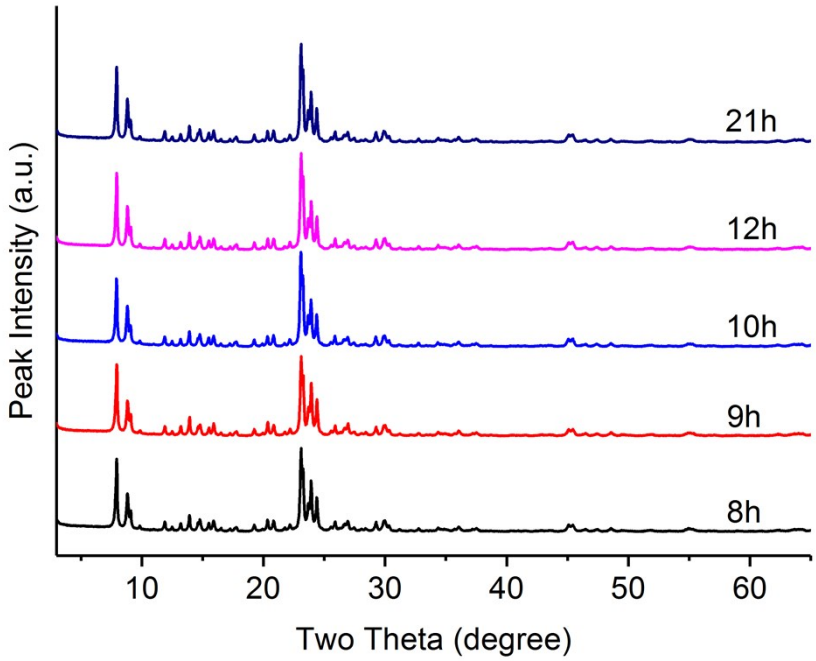


**Figure S17** XRD patterns of zeolites obtained after different times of hydrothermal synthesis.

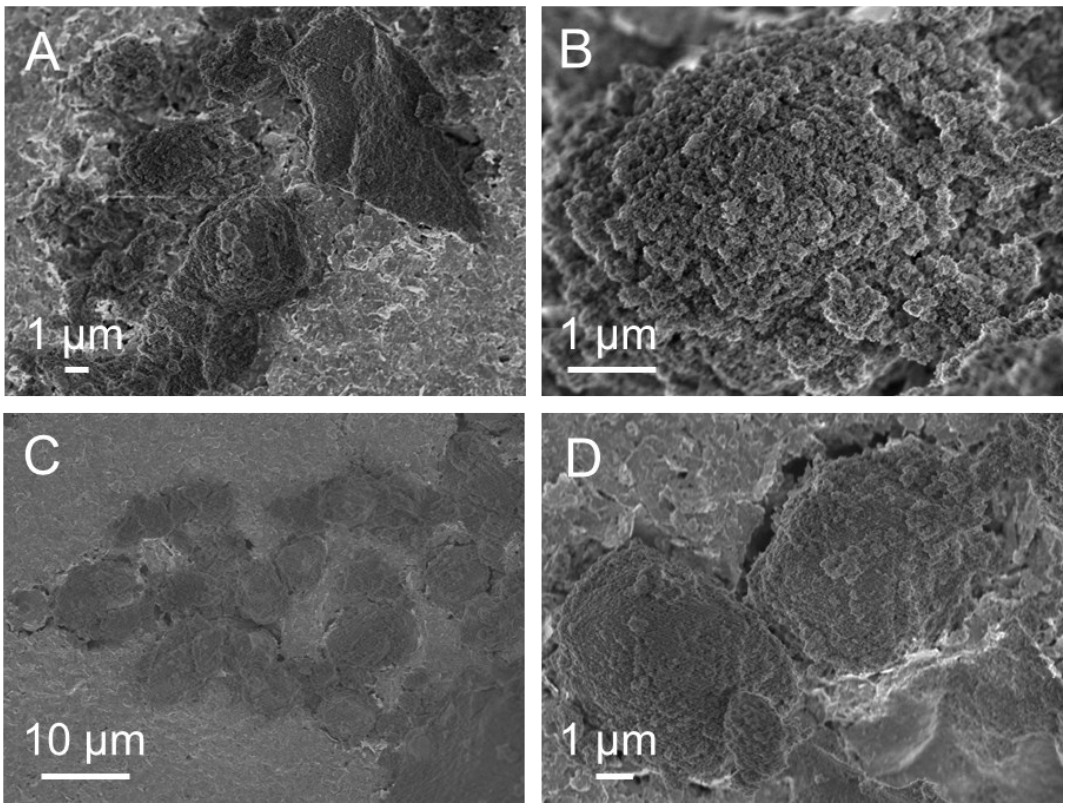


**Figure S18** SEM images of samples collected after hydrothermal synthesis for 6h (A, B) and 8h (C, D).

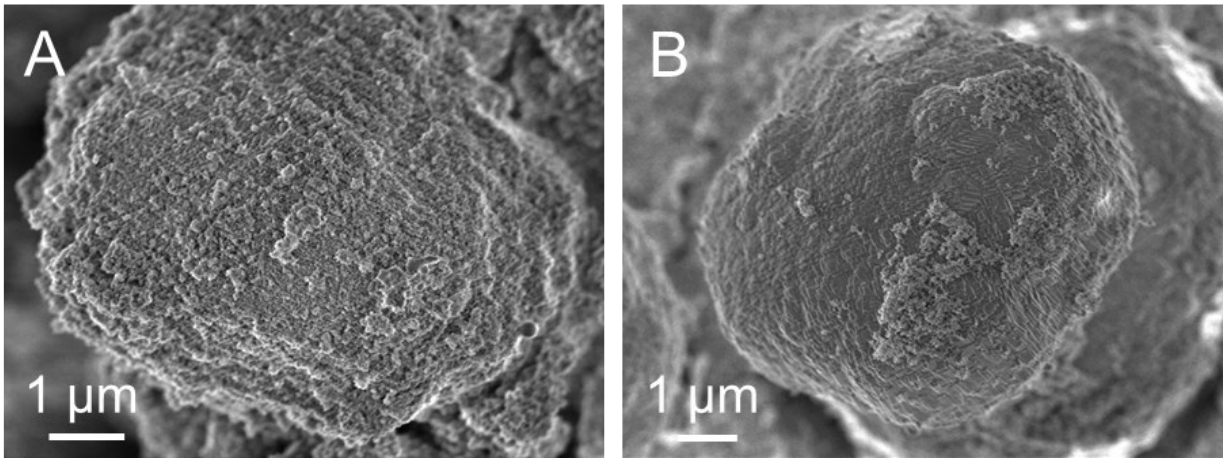


**Figure S19** SEM images showing the morphology change of zeolite particles after hydrothermal synthesis of (A) 9 h and (B) 12 h.

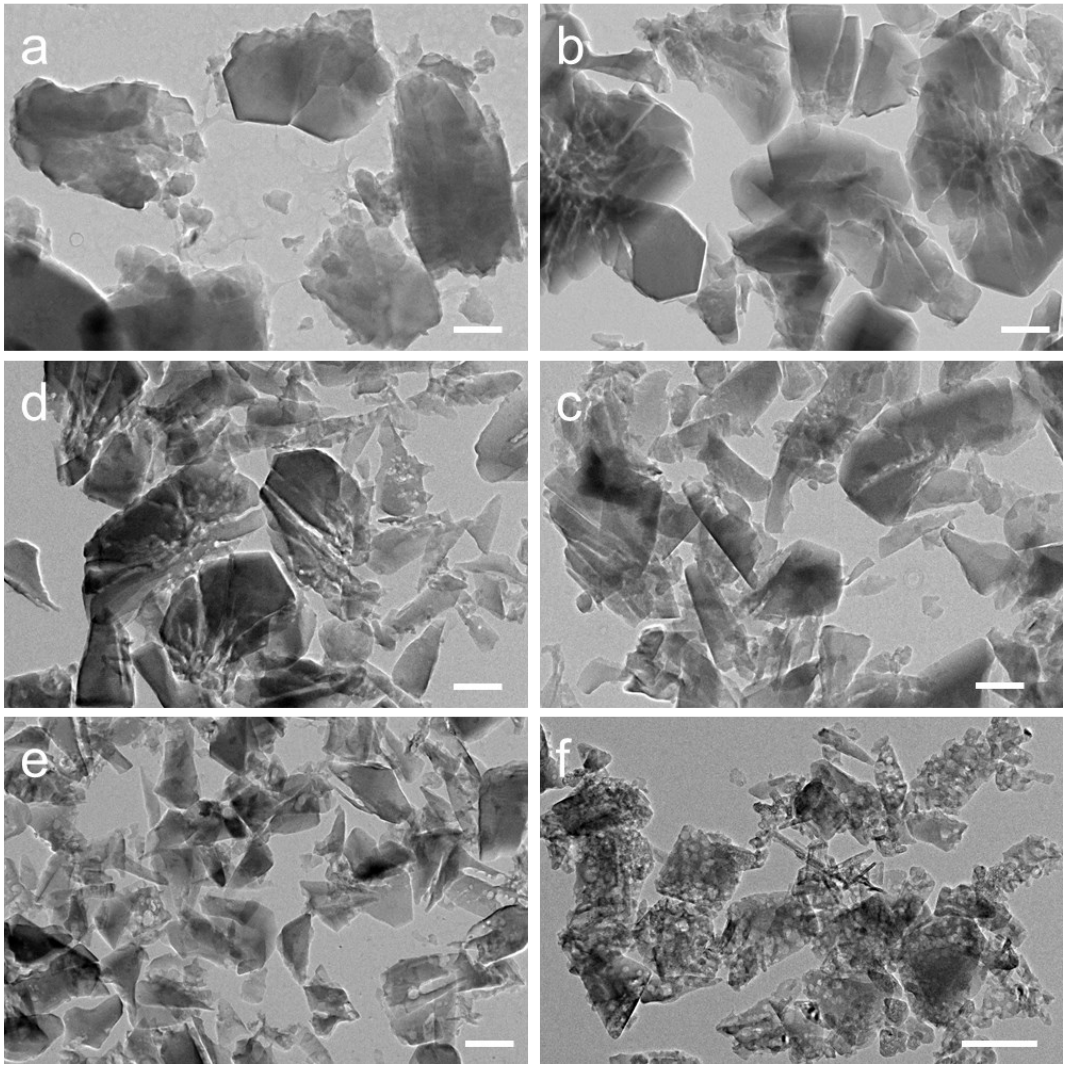


**Figure S20** TEM images of the parent ZSM-5-I from Grace Davison (a), and the samples treated by $NH_4F$ for different time (b: 5 min; c: 10 min; d: 20 min; e: 40 min; f: 60 min), scale bars in a-f are 200 nm. The experimental conditions for the $NH_4F$ etching of $Z_p$ are identical with the fluoride etching of the ZSM-5 sample from Grace Davison.

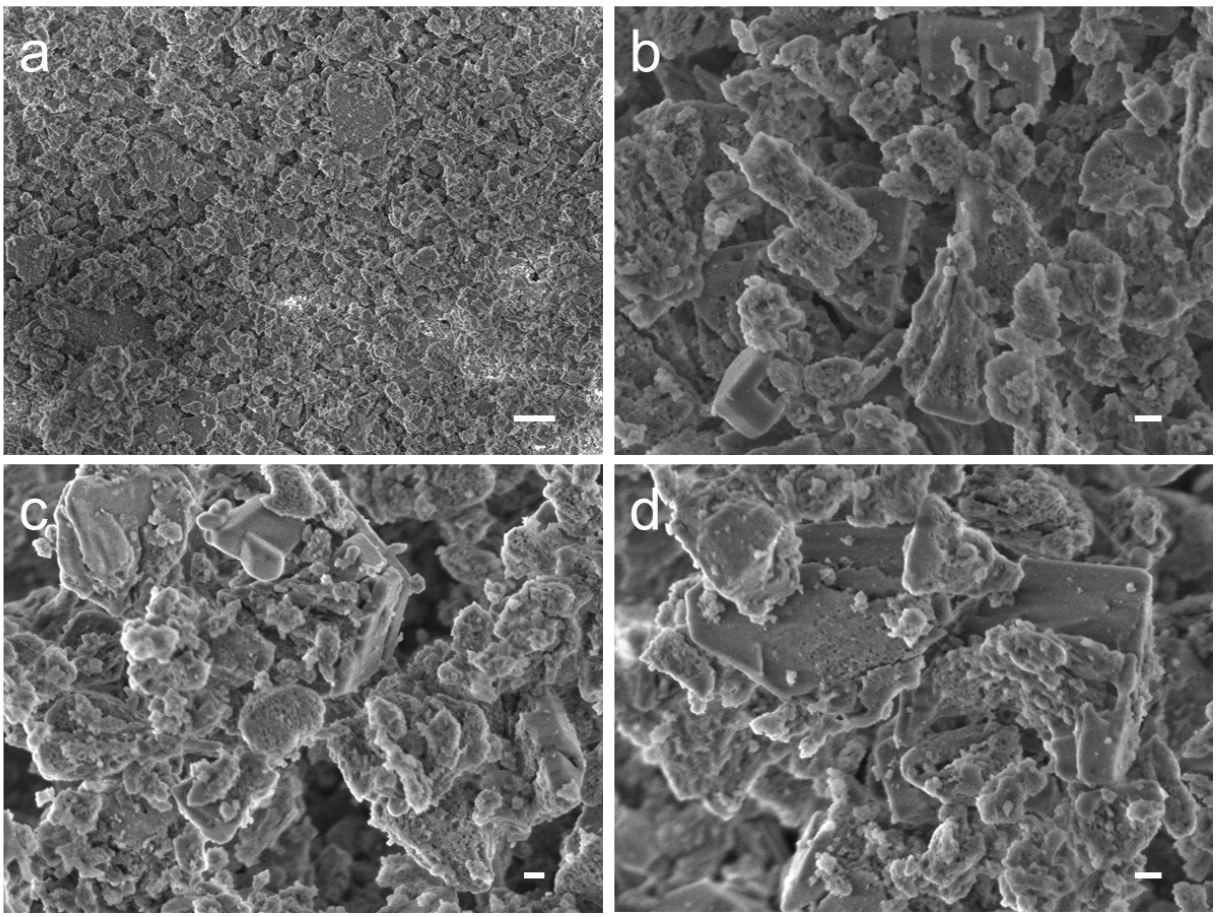


**Figure S21** SEM images at different magnifications showing the defect-zoning of the calcined ZSM-5-H1 zeolite after $NH_4F$ treatment. Scale bars are 100 nm in b-d and 1 μm in a.

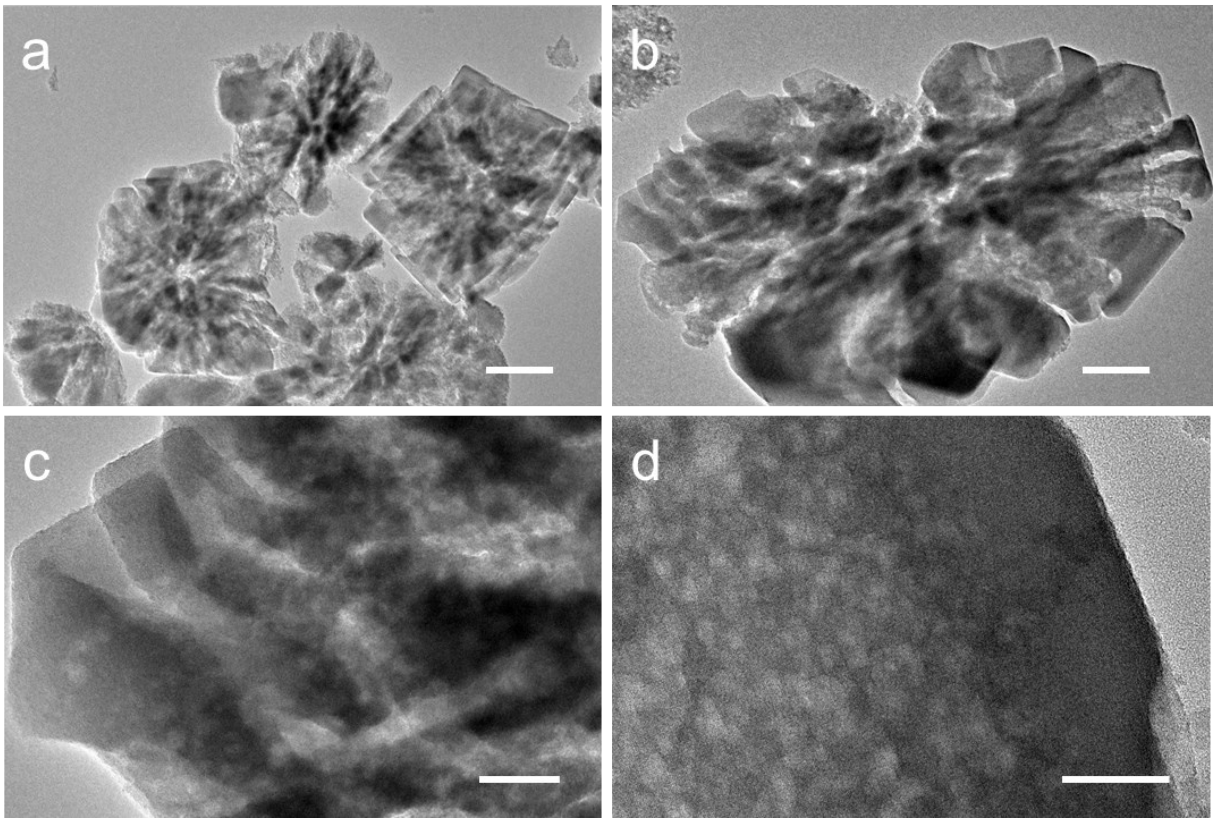


**Figure S22** TEM images at different magnifications showing the defect-zoning of the calcined ZSM-5-H1 zeolite after $NH_4F$ treatment. Scale bars are 500 nm in a, 200 nm in b and 50 nm in c and d.

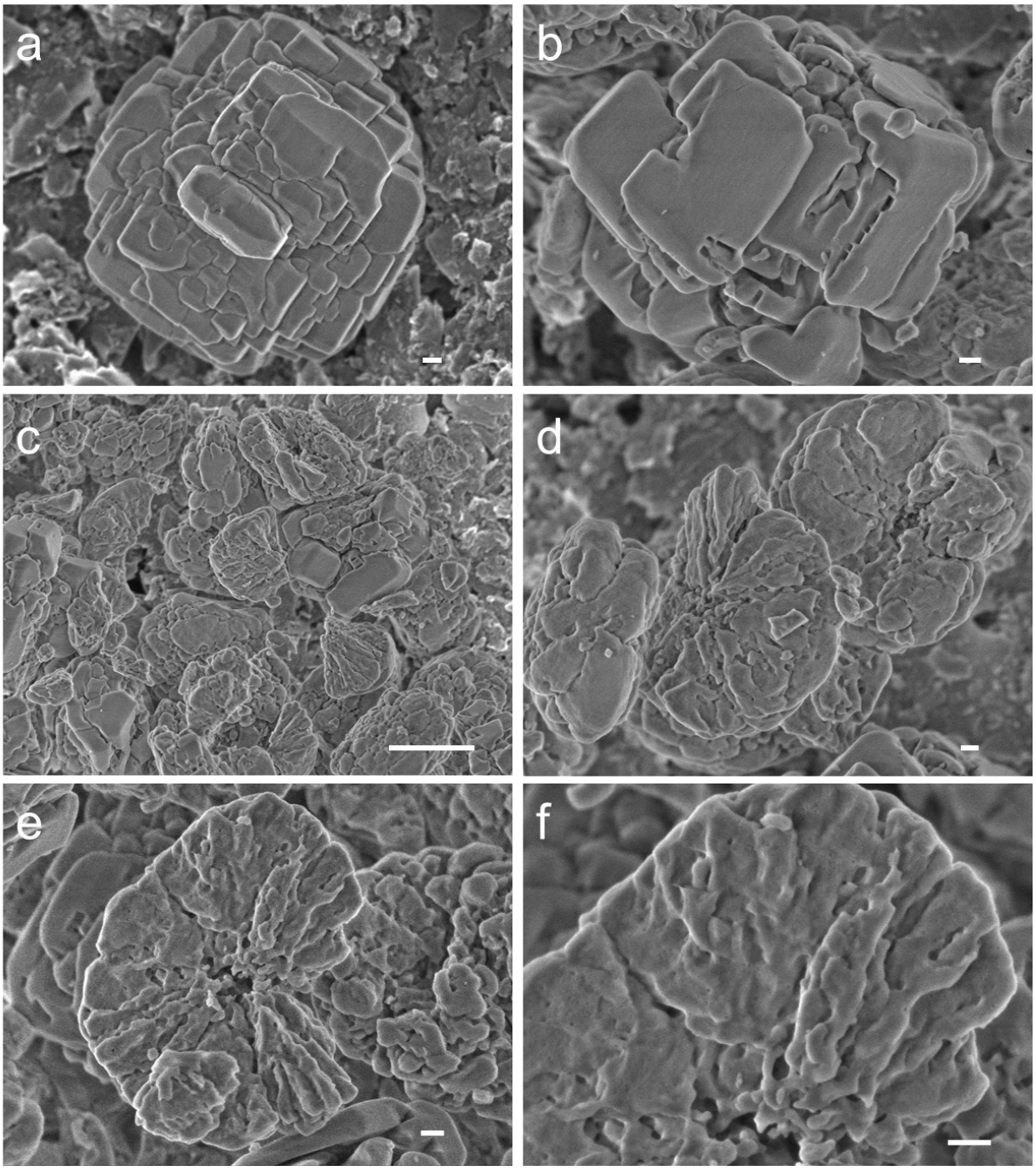


**Figure S23** SEM images of the as-synthesized ZSM-5-H1 zeolite (a) and the $NH_4F$ treated counterparts (b-f) showing the preferential dissolution of zeolite core and the spliting of crystals along extended grain boundaries. The durability of zeolite crystals in $NH_4F$ solution is due to the protection effect of charge and defect sites compensating $TPA^+$. Scale bars are all 100 nm except 1 μm in c.

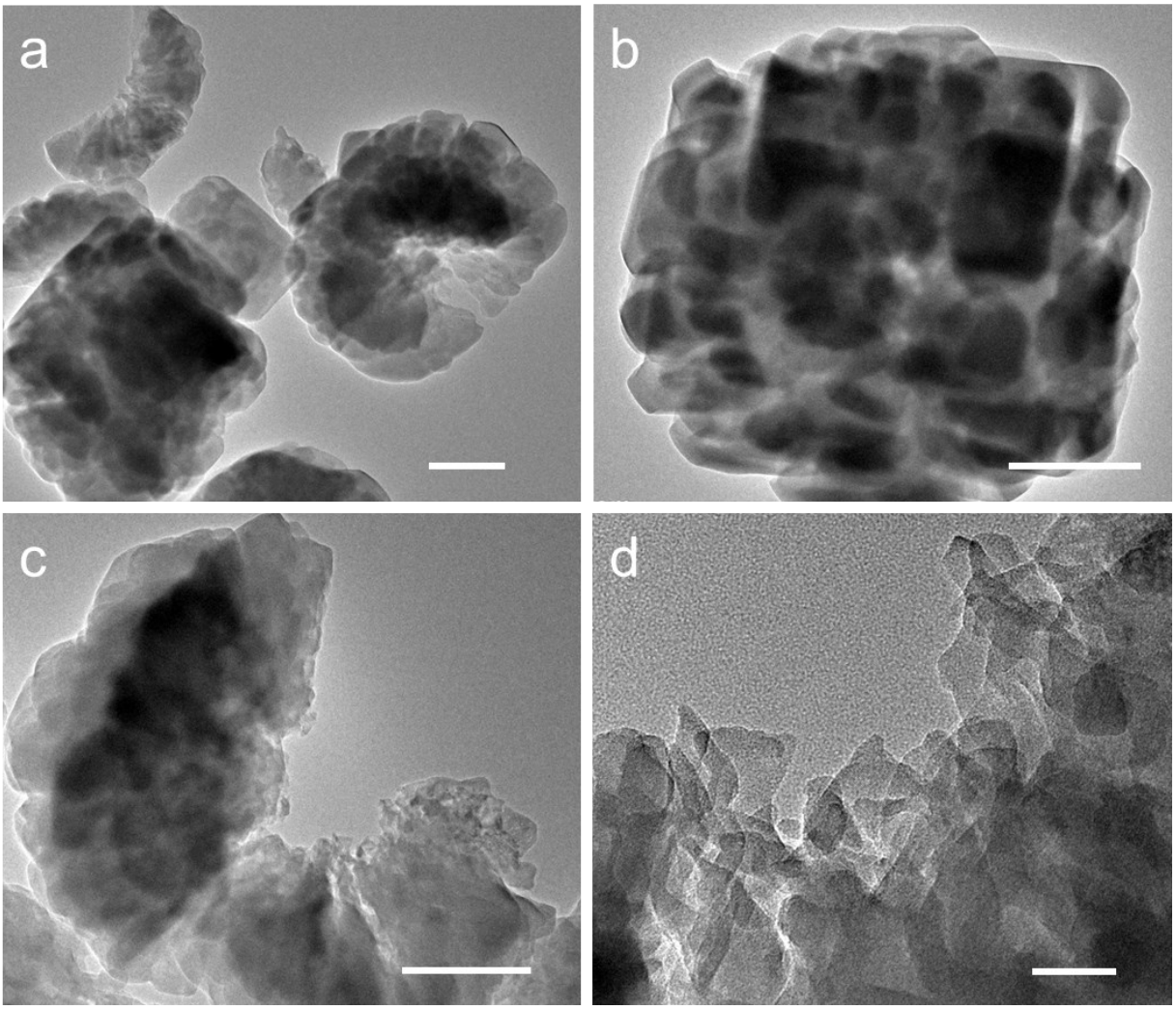


**Figure S24** TEM images of the as-synthesized ZSM-5-H1 zeolite after $NH_4F$ treatment (a-d). Scale bars are 500 nm in a-c, and 50 nm in d.

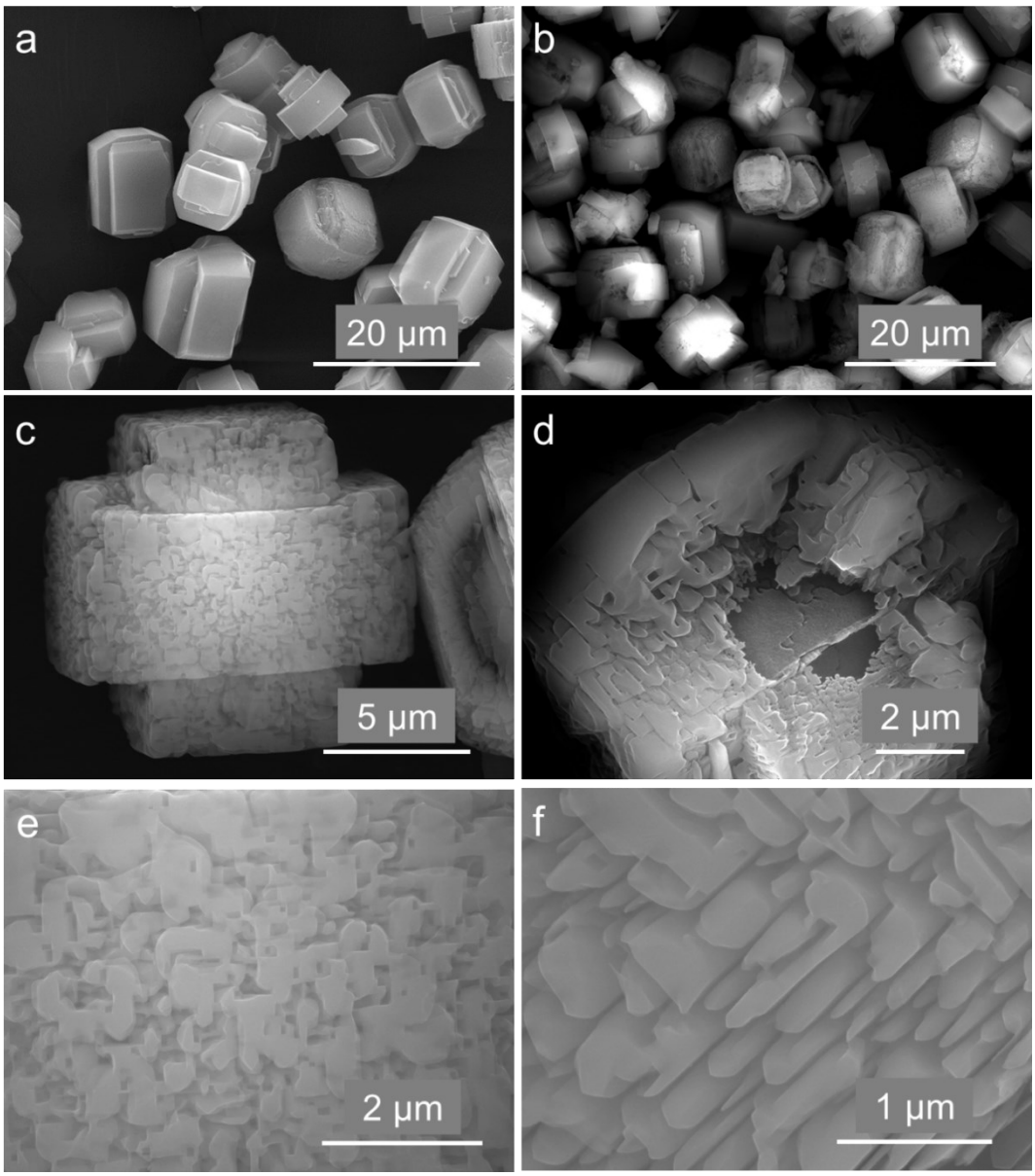


**Figure S25** SEM images of parent (a) and $NH_4F$ treated (b-f) ZSM-5-H2 zeolite at different magnifications showing the dissolution behavior of ZSM-5-H2 under the protection of $TPA^+$.